Stochastic Geometry Based Performance Study on 5G Non-Orthogonal Multiple Access Scheme

Zekun Zhang†, Haijian Sun†,Rose Qingyang Hu†, Yi Qian‡
†Department of Electrical and Computer Engineering, Utah State University, Logan, UT
‡Department of Computer and Electronics Engineering, University of Nebraska-Lincoln, NE
Email: †{zekun.zhang.z@ieee.org, h.j.sun@ieee.org, rosehu@ieee.org}, ‡yqian@ieee.org

***Abstract*—To achieve a significant boost on capacity performance in the next generation (5G) cellular network, novel radio access technologies (RAT) are demanded to make the system more spectrum efficient. As a promising multiple access scheme for 5G cellular network, non-orthogonal multiple access (NOMA) has attracted extensive research attention recently. Existing works show that NOMA posses the potential to further improve system spectrum efficiency compared with the orthogonal multiple access (OMA), which is predominantly adopted by existing wireless networks. In this paper, we develop the analytical framework on system coverage and average user achievable rate in a downlink NOMA system. We explicitly consider the inter-cell interference in the study, which is a capacity limiting factor in most wireless networks but less addressed in most existing analytical work for NOMA. Additional to NOMA, the analysis on an OMA access scheme, i.e., orthogonal frequency division multiple access (OFDMA), is also conducted for comparison. Owing to the tractability of Poisson Point Process (PPP) model used in this work, all the analytical results are derived and expressed in a pseudo-closed form or a succinct closed form. The analytical results are validated by simulations and demonstrate that NOMA can bring considerable performance gain compared to OMA when success interference cancellation (SIC) error is low.**

***Index Terms*—5G, NOMA, PPP, coverage probability, average achievable rate**

I. INTRODUCTION

Orthogonal multiple access (OMA) has been widely applied in current wireless communications systems, such as orthogonal frequency division multiple access (OFDMA) or single carrier frequency division multiple access (SC-FDMA) adopted in Long-Term Evolution (LTE) [1] and LTE-Advanced [2]. Although OMA eliminates inter-user interference with a low-complexity implementation, its spectrum efficiency has room to be further improved [3]. One of the most challenging requirements in the next generation (5G) cellular network is to offer data rate 1000 $\times$ of the current 4G technology [4]. As such, novel radio access technologies (RAT) with higher spectral efficiency are expected.

Non-orthogonal multiple access (NOMA), as a promising candidate RAT in 5G network, has received considerable attention recently [5]–[8]. Specifically, NOMA allocates the same frequency/time/spatial resource to multiple user equipments (UEs) by multiplexing these UEs on the power domain at the transmitter and extracting the intended signals from the composite data using successive interference cancellation (SIC) at the receiver [9]. Many problems about NOMA have been studied by published work. In [10], authors considered user fairness in the downlink NOMA and investigated power allocation (PA) techniques that ensure fairness for users. Authors of [11] investigated the system level performance of NOMA in various environments including macro cells and small cells, and showed that the performance gain of NOMA can be obtained in both macro cell and small cell deployments. In [12], the performance of a cellular network that jointly considers multiuser multi-input multi-output (MU-MIMO) and NOMA with underlaid device-to-device (D2D) communications is studied. In [13], authors proposed two user pairing schemes and investigated how to further enhance the performance gain of NOMA over conventional OMA.The study shows that NOMA can be applied on both downlink and uplink [14].

To the best of our knowledge, [6] is the only one that focuses on evaluating the performance of NOMA by using the stochastic geometry method. Authors in [6] developed analytical results on outage probability for m-th UE and of the ergodic sum rate in a single cell downlink NOMA. However, due to less tractability of the model used in [6], the clear closed form expression for the ergodic sum rate is difficult to derive. Moreover, inter-cell interference, which is a pervasive problem in most of the existing wireless networks, is not explicitly considered in [6] and neither do many other work on NOMA. In this paper, we evaluate the performance of downlink NOMA on coverage probability and average achievable rate using a stochastic geometry model. More specifically, Poisson Point Process (PPP) model is used in the study. The advantages of adopting PPP model are summarized in [15]: i) It models the real network deployment quite accurate; ii) Inter-cell interference can be explicitly considered; iii) It provides tractable and accurate results. Without loss of generality, we start our analysis with a 2-UE NOMA case and further extend the results to a general M-UE NOMA scenario. Owing to the tractability of PPP model, all the analytical results are expressed in a pseudo-closed form with computable numerical integration, or in a nice closed form under some special cases. We expect our developed work can be used as a frame work for downlink NOMA and to incorporate more advanced schemes such as optimal NOMA power allocation and user pairing.

The rest of the paper is organized as follows. In section II the system model and configurations are lay out. In section III, we derive the statistical coverage probability and average achievable rate for NOMA UEs. The analytical results for

978-1-5090-1328-9/16/$31.00 ©2016 IEEE

OMA UEs are also provided in this section to make a comparison. In section IV, performance results from both analysis and simulations are presented. Finally conclusions are drawn in section V.

II. SYSTEM MODEL

In this paper we consider a multi-cell downlink cellular network. The location of Base Stations (BSs) follows a 2-D homogeneous PPP Φ with a density λ. We assume each UE is associated with the closest BS, which means UEs associated to a BS are located in the Voronoi cell of the associated BS as shown in Fig. 1. The transmission distance between UE_i and its associated BS is denoted by r_i. For all UEs, $\{r_i\}$ is independently and identically distributed (i.i.d.) with a probability density function (pdf) given in [15] as $f_{r_i}(r_i) = e^{-\lambda\pi r_i^2} 2\pi\lambda r_i$. The reuse factor of the system under study is 1. Hence all the cells have the same radio resources and we can normalize the cell resources to 1. We assume an interference limited wireless system given an dense deployment of small cells and hence the impact of noise is neglected throughout the paper. All BSs transmit at the power P_{total}. We adopt a channel model that comprises standard path-loss and Rayleigh fading. $c_i = \frac{h_i r_i^{-\alpha}}{I_i}$ is defined as the channel gain of UE_i normalized by interference, where $h_i \sim \exp(1)$ denotes Rayleigh fading gain and $r_i^{-\alpha}$ corresponds to path-loss. $\alpha > 2$ is the path-loss exponent and $I_i = \sum_{j\in\Phi/b_o} g_j R_{j,i}^{-\alpha} P_{total}$ is the sum of the inter-cell interference from all other BSs, where g_j and $R_{j,i}$ are the Rayleigh fading gain of interfering channel and transmission distance form BS j to UE_i, respectively. Without loss of generality, a NOMA group consists of M UEs, which are sorted based on their normalized channel gain in an ascending order as $c_1 \leq \cdots \leq c_M$. Based on this order, NOMA scheme can allow UE_i to decode the interfering NOMA signals from UE_m, $m \leq i$, and then remove the interfering NOMA signals from the received signal, in a successive manner. Assume the transmission power of UE_i is P_i with $\sum_{i\in M} P_i = P_{total}$. According to the principle of NOMA and the order of UE channel gains, P_i is allocated in a descending order, i.e., $P_1 \geq \cdots \geq P_M$, which is reverse to the order of c_i.

III. COVERAGE PROBABILITY AND AVERAGE ACHIEVABLE RATE

In this section, the coverage probability for each UE in a tagged cell is analyzed. After that we further compute the average achievable rate by using the derived analytical results. For simplicity, we start our analysis with a 2-UE NOMA case and further on extend the results to a general NOMA scheme with M UEs, $M \geq 2$. We denote the signals intended to UE_1 and UE_2 as x_1 and x_2, respectively, where $\mathbb{E}[|x_i|^2] = 1$. According to NOMA principle [5], the transmitted signal at BS is coded as the composite signal from UE_1 and UE_2,

$$x = \sqrt{P_1}x_1 + \sqrt{P_2}x_2. \tag{1}$$

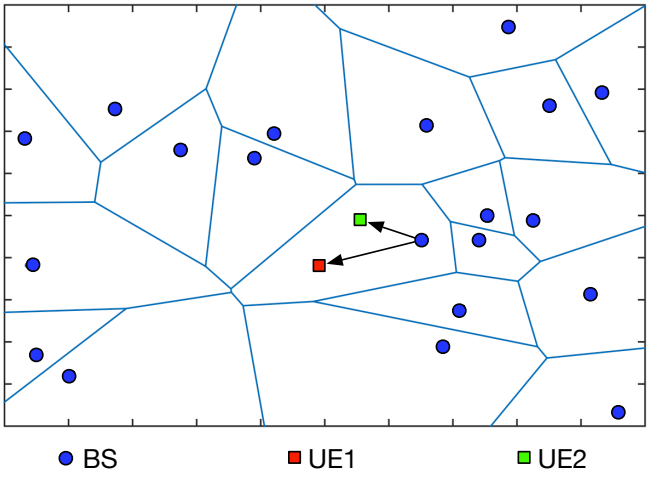

Fig. 1. System Model

Thus the received signal at UE_i can be represented in an interference limited system as

$$y_i = \sqrt{h_i r_i^{-\alpha}}x + I_i. \tag{2}$$

The coverage probability is defined as $\mathbb{P}[SIR > T]$, which represents the probability that the instantaneous signal-to-interference ratio (SIR) of any UE is greater than a certain threshold T. It can also be understood as the complementary cumulative distribution function (CCDF) of SIR over the entire network. The SIR used here is different from the definition of SIR in OMA. Other than the real SIR at the receiving antenna of a UE, we are more interested in the SIR after SIC that can be used to calculate the average achievable rate. Here we name the SIR after SIC as NOMA SIR throughout the paper. In the 2-UE case, UE_1 does not need to perform interference cancellation and directly treats x_2 as interference since it comes the first in the decoding order. UE_2 first decodes x_1 and removes it from the received composite signal y_2, based on which UE_2 can further decode x_2. Assuming successful decoding and no error propagation, the NOMA SIR of UE_1 and UE_2 can be respectively expressed as

$$SIR_1 = \frac{h_1 r_1^{-\alpha} P_1}{I_1 + h_1 r_1^{-\alpha} P_2}, \quad SIR_2 = \frac{h_2 r_2^{-\alpha} P_2}{I_2}. \tag{3}$$

A. Channel Gain Distribution

To evaluate the coverage probability, we need to first derive the channel gain distribution. For a given normalized channel gain $c = \frac{h r^{-\alpha}}{I}$, where h, r and I are the corresponding components as defined before by removing the subscripts, the cumulative distribution function (cdf) is $F_c(C) = \mathbb{P}[c \leq C] = 1 - \mathbb{P}[c > C]$. By following the similar way presented in [15], the complete expression of $\mathbb{P}[c > C]$ is given below.

$$\begin{aligned}\mathbb{P}[c>C] &= \mathbb{E}_r[\mathbb{P}[c>C|r]] \\ &= \int_{r>0} \mathbb{P}\Big[\frac{hr^{-\alpha}}{I} > C\Big|r\Big] f_r(r)dr \\ &= \int_{r>0} \mathbb{E}_I[\mathbb{P}[h>Cr^{\alpha}I|r,I]] f_r(r)dr \\ &\overset{(a)}{=} \int_{r>0} \mathbb{E}_I[\exp(-Cr^{\alpha}I)|r,I] f_r(r)dr \\ &= \int_{r>0} \mathcal{L}_I(Cr^{\alpha}) f_r(r)dr, \end{aligned} \tag{4}$$

where (a) follows from $h \sim \exp(1)$. $\mathcal{L}_I(s) = \mathbb{E}_I[e^{-sI}]$ is the Laplace transform of random variable I evaluated on s. The full expression of $\mathcal{L}_I(s)$ is given by

$$\begin{aligned}&\mathcal{L}_I(s) \\ &= \mathbb{E}_{\Phi,g}\Big[\exp(-s\sum_{j\in\Phi/b_o} g_j R_j^{-\alpha} P_{total})\Big] \\ &= \mathbb{E}_{\Phi}\Big[\prod_{j\in\Phi/b_o} \mathbb{E}_{g_j}[\exp(-sg_j R_j^{-\alpha} P_{total})]\Big] \\ &\overset{(a)}{=} \exp\Big(-2\pi\lambda\int_r^{\infty}\big(1-\mathbb{E}_g[\exp(-sgv^{-\alpha}P_{total})]\big)vdv\Big) \\ &\overset{(b)}{=} \exp\Big(-2\pi\lambda\int_r^{\infty}\big(1-\frac{1}{1+sv^{-\alpha}P_{total}}\big)vdv\Big) \\ &= \exp\Big(-2\pi\lambda\int_r^{\infty}\frac{1}{1+\frac{v^{\alpha}}{sP_{total}}}vdv\Big) \\ &\overset{(c)}{=} \exp\Big(-\pi\lambda(sP_{total})^{\frac{2}{\alpha}}\int_{\frac{r^2}{(sP_{total})^{\frac{2}{\alpha}}}}^{\infty}\frac{1}{1+u^{\frac{\alpha}{2}}}du\Big). \end{aligned} \tag{5}$$

In the above (a) follows from the probability generating functional (PGFL) of PPP [16], which states that $\mathbb{E}[\prod_{x\in\Phi} f(x)] = \exp(-\lambda\int_{\mathbb{R}^2}(1-f(x))dx)$. (b) follows from $g \sim \exp(1)$ and (c) is acquired by change of variable $u = \frac{v^2}{(sP_{total})^{\frac{2}{\alpha}}}$. By substituting $s = Cr^{\alpha}$ back into (5), we can get the complete expression of $\mathcal{L}_I(Cr^{\alpha})$ as

$$\mathcal{L}_I(Cr^{\alpha}) = \exp\Big(-\pi\lambda r^2(CP_{total})^{\frac{2}{\alpha}}\int_{(CP_{total})^{-\frac{2}{\alpha}}}^{\infty}\frac{1}{1+u^{\frac{\alpha}{2}}}du\Big). \tag{6}$$

Combining (6) with (4) and using $f_r(r) = e^{-\lambda\pi r^2}2\pi\lambda r$, we can write the following.

$$\begin{aligned}&\mathbb{P}[c>C] \\ &= \int_{r>0}\exp\Big(-\pi\lambda r^2(CP_{total})^{\frac{2}{\alpha}}\int_{(CP_{total})^{-\frac{2}{\alpha}}}^{\infty}\frac{1}{1+u^{\frac{\alpha}{2}}}du\Big) \\ &\quad\cdot e^{-\lambda\pi r^2}2\pi\lambda r dr \\ &\overset{(a)}{=} \int_{v>0} e^{\left(-v\pi\lambda(1+(CP_{total})^{\frac{2}{\alpha}}\int_{(CP_{total})^{-\frac{2}{\alpha}}}^{\infty}\frac{1}{1+u^{\frac{\alpha}{2}}}du)\right)}\pi\lambda dv \\ &= \frac{1}{1+(CP_{total})^{\frac{2}{\alpha}}\int_{(CP_{total})^{-\frac{2}{\alpha}}}^{\infty}\frac{1}{1+u^{\frac{\alpha}{2}}}du}, \end{aligned} \tag{7}$$

where (a) uses $v = r^2$. Finally we derive the cdf of the channel gain as

$$F_c(C) = 1 - \frac{1}{1+(CP_{total})^{\frac{2}{\alpha}}\int_{(CP_{total})^{-\frac{2}{\alpha}}}^{\infty}\frac{1}{1+u^{\frac{\alpha}{2}}}du}. \tag{8}$$

For a special case with $\alpha = 4$, (8) can be further simplified to

$$F_c(C) \overset{\alpha=4}{=} 1 - \frac{1}{1+\sqrt{CP_{total}}(\frac{\pi}{2} - \arctan(\frac{1}{\sqrt{CP_{total}}}))}. \tag{9}$$

Knowing only the cdf of the channel gain is sufficient to compute the UE coverage probability in our system model. The pdf of channel gain is also presented for any further NOMA study based on this framework. By taking the derivative on $F_c(c)$, the pdf can be found as

$$\begin{aligned} f_c(c) &= \frac{dF_c(c)}{dc} \\ &= \frac{\mu(c)'\nu(c) + \mu(c)\nu'(c)}{1+2\mu(c)\nu(c)+\mu(c)^2\nu(c)^2}, \end{aligned} \tag{10}$$

where

$$\mu(c) = (cP_{total})^{\frac{2}{\alpha}}, \quad \mu'(c) = \frac{d\mu(c)}{dc} = \frac{2}{\alpha}P_{total}^{\frac{2}{\alpha}}c^{\frac{2}{\alpha}-1},$$

$$\nu(c) = \int_{(cP_{total})^{-\frac{2}{\alpha}}}^{\infty}\frac{1}{1+u^{\frac{\alpha}{2}}}du,$$

$$\nu'(c) = \frac{d\nu(c)}{dc} = \frac{2P_{total}}{\alpha(cP_{total})^{\frac{2}{\alpha}}(1+cP_{total})}.$$

B. NOMA Coverage for the 2-UE case

In this subsection we study the coverage probability for UE_1 and UE_2 in a 2-UE NOMA case. We randomly select two UEs among all UEs associated with the tagged BS and mark them as UE_a and UE_b. The two UEs are ranked based on their channel gains in an ascending order. After sorting, the subscript of two selected UE will be remarked as $UE_1 = \{UE_i | UE_i \in \{UE_a, UE_b\}, c_i = \min(c_a, c_b)\}$ and $UE_2 = \{UE_i | UE_i \in \{UE_a, UE_b\}, c_i = \max(c_a, c_b)\}$. Now $c_1 = \min(c_a, c_b)$ and $c_2 = \max(c_a, c_b)$, which follows the order rule as $c_1 \le c_2$. Based on [17], for $z = \max(x, y)$ and $w = \min(x, y)$, the cdf of z and w can be determined as $F_z(z) = F_{xy}(z, z)$ and $F_w(w) = F_x(w) + F_y(w) - F_{xy}(w, w)$. Thus we can obtain the cdf of c_1 and c_2 as follows.

$$\begin{aligned} F_{c_1}(c_1) &= F_{c_a}(c_1) + F_{c_b}(c_1) - F_{c_a c_b}(c_1, c_1) \\ &= 2F_c(c_1) - F_c(c_1)^2. \end{aligned} \tag{11}$$

$$F_{c_2}(c_2) = F_{c_a c_b}(c_2, c_2) = F_c(c_2)^2. \tag{12}$$

We use the fact that $\{c_i\}$ is i.i.d. and $F_c(c)$ is given in (8). For a target SIR value of T, the coverage probability of UE_1 is

$$\begin{aligned}\mathbb{P}[SIR_1 > T] &= 1 - \mathbb{P}[SIR_1 \le T] \\ &= 1 - \mathbb{P}\Big[\frac{h_1 r_1^{-\alpha} P_1}{I_1 + h_1 r_1^{-\alpha} P_2} \le T\Big] \\ &= 1 - \mathbb{P}\Big[\frac{1}{\frac{I_1}{h_1 r_1^{-\alpha} P_1} + \frac{P_2}{P_1}} \le T\Big] \\ &= 1 - \mathbb{P}\Big[\frac{I_1}{h_1 r_1^{-\alpha} P_1} \ge \frac{1}{T} - \frac{P_2}{P_1}\Big]. \end{aligned} \tag{13}$$

Due to NOMA inter-user interference, SIR_1 has an upper bound as $\lim_{I_1\to 0} SIR_1 = \frac{P_1}{P_2}$. So $\mathbb{P}[SIR_1 > T] = 0$ when $T \geq \frac{P_1}{P_2}$. When $T < \frac{P_1}{P_2}$, we continue our derivation

$$\begin{aligned}\mathbb{P}[SIR_1 > T] &= 1 - \mathbb{P}\Big[\frac{h_1 r_1^{-\alpha}}{I_1} \leq \frac{1}{\big(\frac{1}{T} - \frac{P_2}{P_1}\big)P_1}\Big] \\ &= 1 - \mathbb{P}\Big[c_1 \leq \frac{1}{\big(\frac{1}{T} - \frac{P_2}{P_1}\big)P_1}\Big] \\ &= 1 - F_{c_1}\bigg(\frac{1}{\frac{P_1}{T} - P_2}\bigg). \end{aligned} \tag{14}$$

The coverage probability of UE_2 can be acquired following the same method above hence the result is given directly without details for derivation. Assume the NOMA inter-user interference form UE_1 is completely eliminated by SIC at UE_2. There is no such a limitation on SIR_2, as on SIR_1.

$$\mathbb{P}[SIR_2 > T] = 1 - F_{c_2}\bigg(\frac{T}{P_2}\bigg). \tag{15}$$

For a general α, the coverage probability of UE_i is in a quasi-closed form due to the numerical integration included in (8). When $\alpha = 4$, a nice closed form expression can be acquired by employing (9) instead of (8).

C. Average Achievable Rate for 2-UE case

In this subsection, we compute the average achievable rate of UE_i in units of nats/Hz (1 bit = $\ln(2)$ =0.693 nats). We assume all UEs use an adaptive modulation and coding so that they can achieve Shannon bound for their instantaneous SIR, i.e. $\ln(1 + SIR)$. τ_i denotes the average achievable rate of UE_i. For UE_1, we have

$$\begin{aligned}&\tau_1 \triangleq \mathbb{E}[\ln(1 + SIR_1)] \\ &= \int_{c_1>0} \mathbb{E}\Big[\ln\Big(1 + \frac{h_1 r_1^{-\alpha} P_1}{I_1 + h_1 r_1^{-\alpha} P_2}\Big)\Big] f_{c_1}(c_1) dc_1 \\ &\overset{(a)}{=} \int_{c_1>0}\int_{t>0} \mathbb{P}\Big[\ln\Big(1 + \frac{h_1 r_1^{-\alpha} P_1}{I_1 + h_1 r_1^{-\alpha} P_2}\Big) > t\Big] dt \cdot f_{c_1}(c_1) dc_1 \\ &\overset{(b)}{=} \int_{c_1>0}\int_{t=0}^{\ln(\frac{P_1}{P_2}+1)} \mathbb{P}\Big[\frac{h_1 r_1^{-\alpha} P_1}{I_1 + h_1 r_1^{-\alpha} P_2} > e^t - 1\Big] dt \cdot f_{c_1}(c_1) dc_1 \\ &= \int_{t=0}^{\ln(\frac{P_1}{P_2}+1)} \bigg(1 - F_{c_1}\Big(\frac{1}{\frac{P_1}{e^t-1} - P_2}\Big)\bigg) dt, \end{aligned} \tag{16}$$

where (a) follows from $\mathbb{E}[X] = \int_{t>0} \mathbb{P}(X > t) dt$ for a positive random variable X and (b) follows from $\lim_{I_1\to 0} \ln(1 + \frac{h_1 r_1^{-\alpha} P_1}{I_1 + h_1 r_1^{-\alpha} P_2}) = \ln(\frac{P_1}{P_2} + 1)$. The achievable average rate of UE_2, τ_2, can be derived in the same way.

$$\tau_2 = \int_{t>0} \Big(1 - F_{c_2}\big(\frac{e^t - 1}{P_2}\big)\Big) dt. \tag{17}$$

D. Coverage Probability and Average Achievable Rate for the M-UE case

By observing the expression of coverage probability and achievable average rate for UE_1 and UE_2 in the 2-UE case, we can extend our results into a general M-UE NOMA scenario. The SIR of UE_i in an M-UE scenario can be expressed as

$$\begin{aligned} SIR_i &= \frac{h_i r_i^{-\alpha} P_i}{I_i + h_i r_i^{-\alpha} \sum_{j=i+1}^{M} P_j} \\ &= \frac{1}{\frac{1}{c_i P_i} + \frac{\sum_{j=i+1}^{M} P_j}{P_i}}. \end{aligned} \tag{18}$$

Notice that $\sum_{j=i+1}^{M} P_j = 0$ when $i = M$. There is an upper bound for all $SIR_i, i \neq M$ as $\lim_{I_i\to 0} SIR_i = \frac{P_i}{\sum_{j=i+1}^{M} P_j}$. So for $T > \frac{P_i}{\sum_{j=i+1}^{M} P_j}$, the coverage probability of UE_i is 0 and for $T \leq \frac{P_i}{\sum_{j=i+1}^{M} P_j}$, the expression can be derived by following the same method applied on the 2-UE case. The complete result can be expressed as

$$\mathbb{P}[SIR_i > T] = \begin{cases} 0, & \text{if } T > \frac{P_i}{\sum_{j=i+1}^{M} P_j}; \\ 1 - F_{c_i}\Big(\frac{1}{\frac{P_i}{T} - \sum_{j=i+1}^{M} P_j}\Big), & \text{otherwise.} \end{cases} \tag{19}$$

$F_{c_i}(c_i)$ can be calculated using the knowledge of order statistics [18]. For n independent random variables $X_1, X_2, ..., X_n$ each with cdf P(x), the cdf of mth order statistics $X_{(m)}$ is $F_m(x) = \sum_{i=m}^{n} \binom{n}{i} P^i(x)[1 - P(x)]^{n-i}$. The smallest order statistics $X_{(1)}$ and the highest one $X_{(n)}$ have simpler expressions as $F_1(x) = 1 - [1 - P(x)]^n$ and $F_{(n)}(x) = P^n(x)$. Since $\{c_i\}$ is i.i.d., the cdf of UE_i's channel gain can be expressed as

$$F_{c_i}(c_i) = \sum_{j=i}^{M} \binom{M}{j} F_c(c_i)^j [1 - F_c(c_i)]^{M-j}. \tag{20}$$

Again for the sake of completeness, we also provide the pdf of c_i as

$$f_{c_i}(c_i) = \frac{M!}{(i-1)!(M-i)!} F_c^{i-1}(c_i)[1 - F_c(c_i)]^{M-i} f_c(c_i). \tag{21}$$

By using (19), the average achievable rate can be computed by following the same method we applied in the last subsection. Due to the limitation of coverage probability, the average achievable rate of UE_i also has an upper bound as $\lim_{I_i\to 0} \tau_i = \ln(1 + \frac{P_i}{\sum_{j=i+1}^{M} P_j})$ for $i \neq M$. The complete expression of τ_i is provided below. Notice that when $i = M$, the range of the integration is $(0, \infty)$.

$$\tau_i = \int_{t=0}^{\ln(1+\frac{P_i}{\sum_{j=i+1}^{M} P_j})} \bigg(1 - F_{c_i}\Big(\frac{1}{\frac{P_i}{e^t-1} - \sum_{j=i+1}^{M} P_j}\Big)\bigg) dt. \tag{22}$$

To make a fair comparison between NOMA and conventional OMA, i.e., OFDMA in this study, the coverage probability and average achievable rate when using OMA are also presented. The result for a randomly chosen UE using OMA is published in [15], while our result provided here is for each UE out of M UEs in a cell, which can be understood as a decomposition of the result in [15]. The mean value is given as $\frac{\sum_{i=1}^{M} \tau_i}{M}$. We assume each UE in OMA is assigned an equal amount of

bandwidth and is allocated the same downlink transmission power. The SIR expression, coverage probability and average achievable rate of UE_i using OMA can be acquired by making some simple modification on the previous NOMA analytical results. Thus in the following we give the results directly without going through the details on derivations.

$$SIR_i^{OMA} = \frac{h_i r_i^{-\alpha} P_{total}/M}{\sum_{j\in\Phi/b_o} g_j R_{j,i}^{-\alpha} P_{total}/M} = c_i P_{total}, \quad (23)$$

$$\mathbb{P}[SIR_i^{OMA} > T] = 1 - F_{c_i}(\frac{T}{P_{total}}), \quad (24)$$

$$\tau_i^{OMA} = \frac{1}{M}\int_{t>0} \big(1 - F_{c_i}(\frac{e^t - 1}{P_{total}})\big)dt. \quad (25)$$

IV. Performance Results

Both simulation results and analytical results are presented in this section. The performance of NOMA and OFDMA are compared under various settings. In OFDMA, we assume the frequency resources are allocated equally to two UEs hence each of them will have 0.5 frequency resource as we normalize the overall bandwidth to 1. $\epsilon \in (0.5, 1)$ is used to represent the relationship between P_1 and P_2 in the 2-UE case, i.e., $P_1 = \epsilon P_{total}$ and $P_2 = (1-\epsilon)P_{total}$. $\alpha = 4$ is used in the performance study.

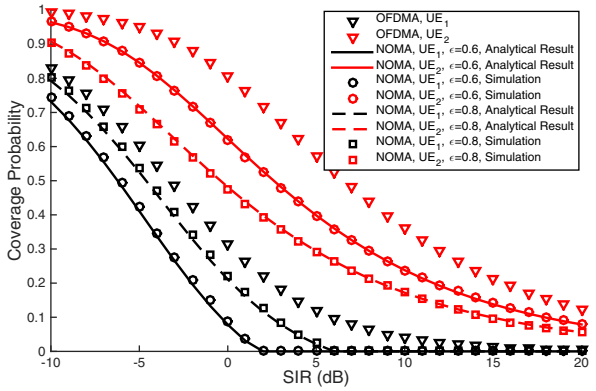

Fig. 2. Coverage probability for OFDMA UE and NOMA UE with different ϵ

Fig. 2 presents the coverage probability for NOMA UEs and OFDMA UEs. The analytical results match simulation results tightly. From the curves, it is clear that there is a trade off between the performance of UE_1 and UE_2 when changing the value of ϵ. When comparing NOMA and OFDMA, for each UE, its coverage probability in the NOMA mode is always worse than its coverage probability in the OFDMA mode due to extra NOMA interference as well as due to a smaller transmission power for the NOMA UE. However, the advantage of NOMA can be observed from the average achievable rate as shown in Fig. 3, which clearly shows that NOMA can achieve a much higher overall sum rate than OFDMA in the most scenarios. We further investigate the impact of power allocation on NOMA by changing ϵ. The average

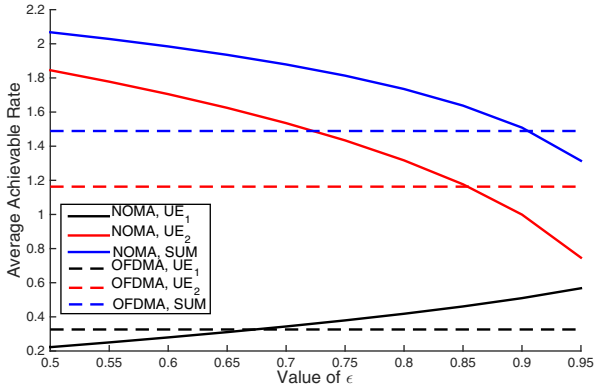

Fig. 3. Average Achievable Rate for OFDMA UE and NOMA UE with different ϵ

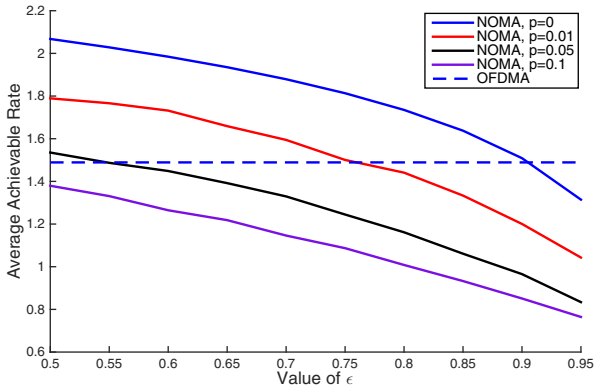

Fig. 4. Average Achievable Rate for NOMA UE with Imperfect SIC

achievable rate under NOMA has an intersection with that under OFDMA for both UE_1 and UE_2 and the intersecting values of ϵ for UE_1 and UE_2 are different. Also we can observe that when $\epsilon \in (0.655, 0.85)$, both UE_1 and UE_2 under NOMA outperform their respective average achievable rate under OFDMA. These observations is useful for seeking the optimal PA scheme aiming at different objectives, i.e., total throughput or user fairness.

In Fig. 4, the impact of imperfect SIC is investigated with simulation results. We use the error propagation model proposed in [19] to model the impact caused by imperfect SIC in NOMA. The degree of SIC error at UE_i is presented by ρ, which is the percentage of inter-user interference that fails to be decoded. For instance, the SIR for UE_2 considering imperfect SIC can be expressed as $SIR_2 = \frac{h_2 r_2^{-\alpha} P_2}{I_2 + \rho h_2 r_2^{-\alpha} P_1}$. From Fig. 4, even 1% unsuccessful decoding will result in more than 10% degradation on average achievable rate. And if ρ reaches 10%, NOMA throughput gain completely disappears regardless of ϵ settings. From this observation, we can conclude that failing to eliminate inter-user interference is fatal to NOMA and can be a challenging issue for implementing NOMA in practice.

In Fig. 5, we investigate the impact of imperfect SIC on the

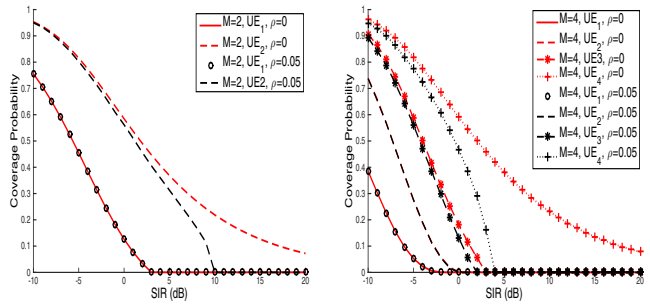

Fig. 5. Coverage Probability for 4-UE and 2-UE NOMA with and without Imperfect SIC

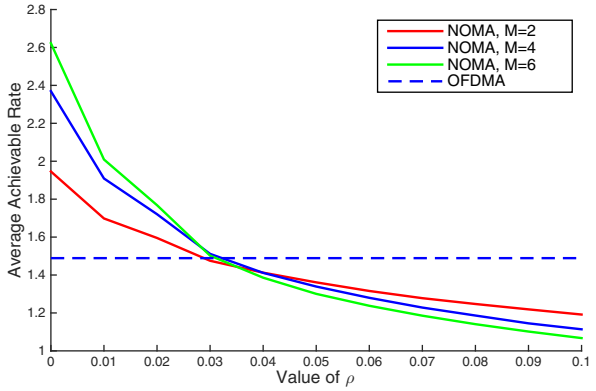

Fig. 6. Average Achievable Rate for 2-UE, 4-UE and 6-UE NOMA with different SIC error ρ

coverage probability for the 4-UE and 2-UE NOMA scenarios. Simulation results are used for comparison and they match the analytical results very well. In each NOMA scenario ($M = 2,\ 4$), UE_i is allocated a power of $P_i = \frac{M-i+1}{\theta}$, where θ is a constant to guarantee $\sum_{i=1}^{M} P_i = P_{total}$. Note that UE_1 is immune to imperfect SIC as it does not need to process any interference cancellation. From Fig. 5, we can observe that UE_M, which comes the last in the decoding order, suffers the most from imperfect SIC as it has the most residual interference if a certain percentage of NOMA inter-user interference, i.e., $\rho \sum_{j=1}^{M-1} P_j$, fails to be decoded. Moreover, P_M is the smallest power among $\{P_i\}$ based on the NOMA power allocation principle and hence makes UE_M even more vulnerable to additional interference. From Fig. 5 we can also see that the impact of imperfect SIC is more significant as M increases. This fact can be observed more clearly from the achievable rate in Fig. 6. The throughput gain of NOMA over OFDMA degrades faster as M increases.

V. CONCLUSIONS

In this paper, we evaluated the performance of NOMA on the coverage probability and average achievable rate by using stochastic geometry method. The analysis explicitly considered inter-cell interference in the model and derived results in a tractable form. The analytical study considers a general M-UE NOMA scheme with flexible power allocation among M UEs. The analytical study are validated by simulation results. The study shows that NOMA in general will degrade UE SIR performance but improves overall system throughout, especially when the NOMA SIC error is low. This work builds a general mathematical framework to evaluate more advanced NOMA schemes in the future.

ACKNOWLEDGMENT

This work was supported by National Science Foundation grants ECCS-1308006, ECCS-1307580, EARS 1547312, and EARS 1547330.

REFERENCES

[1] 3GPP TS36.300, "Evolved Universal Terrestrial Radio Access (E- UTRA) and Evolved Universal Terrestrial Radio Access Network (E- UTRAN)," Overall description.

[2] 3GPP TR36.913 (V8.0.0), "Requirements for further advancements for E-UTRA (LTE-Advanced)," June 2008.

[3] R. Q. Hu and Y. Qian, "An Energy Efficient and Spectrum Efficient Wireless Heterogeneous Network Framework for 5G Systems," *IEEE Communications Magazine*, vol.52, no.5, pp.94-101, May 2014.

[4] J. G. Andrews, S. Buzzi, W. Choi, S. V. Hanly, A. Lozano, A. C. K. Soong, and J. C. Zhang, "What will 5G be?," *IEEE J. Sel. Areas Commun.*, vol. 32, pp. 10651082, Jun. 2014.

[5] Y. Saito, Y. Kishiyama, A. Benjebbour, T. Nakamura, A. Li, and K. Higuchi, "Non-orthogonal multiple access (NOMA) for future radio access," *IEEE VTC*, Spring 2013, June 2013.

[6] Z. Ding, Z. Yang, P. Fan, and H. V. Poor, "On the performance of non-orthogonal multiple access in 5G systems with randomly deployed users," *IEEE Signal Process. Lett.*, vol. 21, no. 12, pp. 15011505, Dec. 2014.

[7] K. Higuchi and A. Benjebbour, "Non-orthogonal Multiple Access (NOMA) with Successive Interference Cancellation for Future Radio Access,"*IEICE Transactions on Communications*, E98.B(3):403-414, Feb. 2015.

[8] A. Benjebbour, Y. Saito, Y. Kishiyama, A. Li, A. Harada, and T.Nakamura, "Concept and practical considerations of non-orthogonal multiple access (NOMA) for future radio access, *IEEE ISPACS*, Nov. 2013.

[9] Mazen O. Hasna et al., "Performance analysis of mobile cellular systems with successive co-channel interference cancellation," *IEEE Trans. on Wireless Commun.*, vol. 2, issue 1, pp. 29-40, February 2003.

[10] S. Timotheou and I. Krikidis, "Fairness for non-orthogonal multiple access in 5G systems," *IEEE Signal Process. Lett.*, vol. 22, no. 10, pp. 1647-1651, Oct. 2015.

[11] Y. Saito, A. Benjebbour, Y. Kishiyama, and T. Nakamura, "Systemlevel performance of downlink non-orthogonal multiple access (NOMA) under various environments," *IEEE VTC*, Spring, May 2015.

[12] H. Sun, Y. Xu, R. Q. Hu, "A NOMA and MU-MIMO Supported Cellular Network with Underlaid D2D Communications," In Proceedings of IEEE VTC Spring 2016.

[13] Z. Ding, P. Fan, and H. V. Poor, "User Pairing in Non-Orthogonal Multiple Access Downlink Transmissions," *IEEE Globecom*, Dec. 2015.

[14] T. Takeda and K. Higuchi, "Enhanced user fairness using non- orthogonal access with SIC in cellular uplink," *IEEE VTC Fall 2011*, Sept. 2011.

[15] J. G. Andrews, F. Baccelli, and R. Ganti, "A tractable approach to coverage and rate in cellular networks," *IEEE Transactions on Communications*, vol. 59, no. 11, pp. 3122-3134, Nov. 2011.

[16] M. Haenggi, "Stochastic geometry for wireless networks." Cambridge University Press, 2012.

[17] A. Papoulis, "Probability, Random Variables, and Stochastic Processes." Fourth Edition.

[18] H. A. David, "Order statistics." John Wiley & Sons Inc, 1970.

[19] H. Sun, B. Xie, R. Q. Hu, G. Wu, "Non-orthogonal Multiple Access with SIC Error Propagation in Downlink Wireless MIMO Networks," accepted to IEEE VTC Fall 2016.